Next generation x-ray optics for astronomy: high resolution, lightweight, and low cost

William W. Zhang, Kim D. Allgood, Michael P. Biskach, Kai-Wing Chan, Michal Hlinka, et al.

William W. Zhang, Kim D. Allgood, Michael P. Biskach, Kai-Wing Chan, Michal Hlinka, John D. Kearney, James R. Mazzarella, Ryan S. McClelland, Ai Numata, Raul E. Riveros, Timo T. Saha, Peter M. Solly, "Next generation x-ray optics for astronomy: high resolution, lightweight, and low cost," Proc. SPIE 11119, Optics for EUV, X-Ray, and Gamma-Ray Astronomy IX, 1111907 (9 September 2019); doi: 10.1117/12.2530284

Event: SPIE Optical Engineering + Applications, 2019, San Diego, California, United States

Next Generation X-ray Optics for Astronomy: High Resolution, Light Weight, and Low Cost

William W. Zhang, Kim D. Allgood[1], Michael P. Biskach[1], Kai-Wing Chan[2], Michal Hlinka[1], John D. Kearney[1], James R. Mazzarella[1], Ryan S. McClelland, Ai Numata[1], Raul E. Riveros[2], Timo T. Saha, and Peter M. Solly[1]

NASA Goddard Space Flight Center, Greenbelt, MD 20771
[1]*also* KBR Inc., Space Engineering Division, Greenbelt, MD 20770
[2]*also* University of Maryland-Baltimore County, Baltimore, MD 21250

ABSTRACT

The capability of an X-ray telescope depends on the quality of its mirror, which can be characterized by four quantities: point-spread-function, photon-collecting area, field of view, and energy bandwidth. In this paper, we report on our effort of developing an X-ray mirror technology that advances all of those four quantities for future X-ray astronomical missions. In addition, we have adopted a modular approach, capable of making mirror assemblies for missions of all sizes, from large missions like *Lynx*, to medium-sized Probes like AXIS, TAP, and HEX-P, to Explorers like STAR-X and FORCE, and to small sub-orbital missions like OGRE. This approach takes into account that all X-ray telescopes must be space-borne and therefore require their mirror assemblies be lightweight. It is designed to make use of modern mass production techniques and commercial off-the-shelf equipment and materials to maximize production throughput and thereby to minimize implementation schedule and costs.

Keywords: X-ray optics, lightweight optics, silicon mirror, meta-shell, x-ray optics

1. INTRODUCTION

Since its beginning with a collimated proportional counter aboard a sounding rocket in the early 1960s, X-ray astronomy has made great progress in the last 50 years. That progress has been largely due to a leap from the use of non-imaging, non-concentrating detectors to the use of focusing optics[1] of progressively higher quality, culminating in the major powerful X-ray observatories such as *Einstein*[2], ROSAT[3], *Chandra*[4], and XMM-*Newton*[5]. Based on the success of those observatories, many next generation X-ray observatories have been proposed and promise to revolutionize our knowledge and understanding of the Universe. In comparison with past and currently operating ones, those new X-ray telescopes have the following characteristics: (1) much better point-spread-function (PSF) to study ever more details of nearby objects and reach further distances in the Universe; (2) much larger photon-collecting area to study ever fainter objects that range in distance from as near as the Moon to as far as the most distant galaxies in the early Universe; (3) much larger field of view (FOV) to gain more contextual information of individual objects and to study diffuse objects that result from the formation of galaxies; and (4) much broader energy bandwidth to detect photons in energy ranging from 0.1 keV to 200 keV, in wavelength from about 124 to 0.06 Angstroms.

The requirements of those future missions, such as *Lynx*[6], AXIS[7], TAP[8], HEX-P[9], STAR-X[10], or FORCE[11], cannot be met with past or existing technologies. Over the last 50 years, many different techniques of making X-ray mirrors have been investigated, with several succeeding in implementing X-ray telescopes. Those successful techniques include the traditional grind-and-polish technique for making the mirrors for *Einstein*, ROSAT, and *Chandra*, the nickel electroforming technique for making the mirrors for *Beppo*SAX[12], XMM-*Newton*, *Swift*[13], and eROSITA[14], the epoxy replication technique for making mirrors for EXOSAT[15] and *Suzaku*[16], and the thermal glass forming technique for making the mirrors for NuSTAR[17]. Each of these techniques has its own advantages and disadvantages. Some of them are capable of making mirrors with excellent PSF, others with light weight, but none can meet the simultaneous requirements of excellent PSF, light weight, large FOV, and broad energy bandwidth.

Optics for EUV, X-Ray, and Gamma-Ray Astronomy IX, edited by Stephen L. O'Dell, Giovanni Pareschi, Proc. of SPIE
Vol. 11119, 1111907 · © 2019 SPIE · CCC code: 0277-786X/19/$21 · doi: 10.1117/12.2530284

The natural geometry of an X-ray mirror assembly is of many concentric shells. Each shell is, in and of itself, a telescope, having the same focal length and co-aligned with others to contribute to the photon-collecting area of the entire mirror assembly. As such, there are two natural ways of implementing an X-ray mirror assembly: the full shell approach in which the basic element of the assembly is an integral shell spanning the entire 360-degree circumference, and the segmented approach in which many mirror segments, each of which covers a fraction of the 360-deg circumference, are precisely aligned and integrated together to make up the entire telescope. *Einstein*, ROSAT, *Chandra*, and XMM-*Newton* were implemented with the full shell approach, while other telescopes with the segmented approach. The two approaches each have its own advantages and disadvantages. Having carefully considered the many factors involved in the making of an X-ray telescope, we have adopted the segmented approach. It is our view that, taking into account the multi-faceted science performance requirements of PSF, photon-collecting area, FOV, and energy bandwidth and practical requirements of mirror production throughput and costs, the advantages of the segmented approach outweigh its disadvantages.

2. TECHNOLOGY PARADIGM

We have adopted a modular approach to building a mirror assembly[18], which is schematically illustrated in Figure 1, consisting of four distinct steps. In the first step, many mirror segments are fabricated. These mirror segments meet specific requirements in terms of dimension, mass, figure, and microroughness. In particular, following the traditional philosophy of making highest quality telescopes, we require that each mirror segment, in and of itself, must meet figure requirements. In the second step, a large number of mirror segments are aligned and bonded to make mirror modules. As in the case of the mirror segment, each module, in and of itself, must meet both science performance and spaceflight environmental requirements. In the third step, a number of mirror modules, each of which has been naturally designed and built to be part of a cylinder, are aligned and integrated to make a meta-shell. In the final step, a number of meta-shells are integrated to make the mirror assembly.

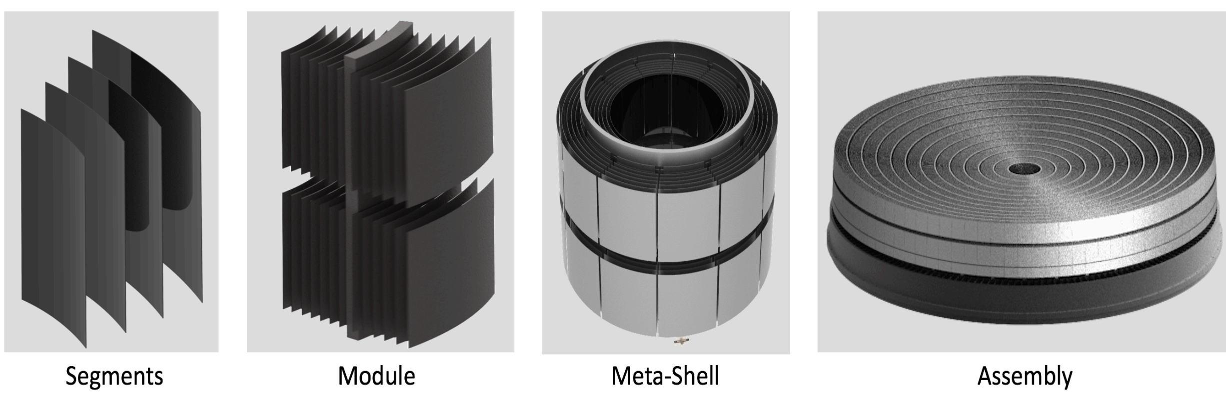

Figure 1. The four steps of building an X-ray mirror assembly for spaceflight. Using as an example the mirror assembly required for the *Lynx* observatory, 37,492 mirror segments will be fabricated. They will be integrated into 611 mirror modules, which in turn will be integrated into 12 meta-shells. The 12 meta-shells will be finally integrated into an assembly. After both science performance and spaceflight environmental testing, the mirror assembly will be integrated to the *Lynx* observatory.

Many considerations have been taken into account to arrive at the above technology paradigm[19-27], both for achieving the best possible science performance and for the purpose of practical implementation in terms of schedule and cost, as well as post-launch operations. This paradigm has many advantages.

First, it clearly delineates the process of building a large and complex mirror assembly into four distinct steps, each of which is self-contained and has well-defined interfaces with others. For technology development, each can be developed and perfected on its own. Depending on availability of resources, these steps can be developed concurrently in parallel and serially one after the other. In particular, this approach separates technology development, the first and second steps, from engineering development, the third and fourth steps.

Second, for implementation, this approach enables the use of mass production techniques to maximize throughput while minimizing schedule and costs. Multiple separate and independent facilities, perhaps in geographically disparate locations, can be used to make the mirror segments and to make the mirror modules, which are then delivered to another facility for integration into meta-shells and a mirror assembly. In particular, the first two steps are highly amenable to the management of spares because of many mirror segments and modules are identical, enabling the use of commercial industry risk management practices to handle those spaceflight hardware pieces, significantly reducing costs.

3. TECHNOLOGY CONSIDERATIONS

Since X-ray telescopes must be space-borne, only the Type-I configuration[28] with both reflections taking place on concave surfaces is practically useful, efficiently utilizing both volume and mass. While the Wolter-Schwarzschild prescription, which fulfills Abbe's sine condition for imaging, is much superior, up until now only the Wolter prescription, where the primary mirror is parabolic and secondary hyperbolic, has been implemented. This is primarily because the image of the telescopes has not been of sufficient quality to benefit from the superior performance of the Wolter-Schwarzschild design and that the grazing incidence nature of X-ray reflection results in field curvature being the dominant aberration. In the case of grazing incidence optics, the field curvature is compounded by two factors. First, the cylindrical nature of the mirror shell itself leads to severe field curvature. Second, the optical pathlength is only preserved within each shell, not across different shells, resulting in each shell having its own unique field curvature. The focal surface of the entire mirror assembly is necessarily an average of the disparate focal surfaces of the many shells optimized under some conditions for a particular energy.

For a given focal length, the field curvature of a shell depends on its radius and its length in the optical axis direction: the shorter the shell length, the smaller the field curvature. On the other hand, the diffraction-limited image quality depends on the shell length in the opposite way: the shorter the shell length, the worse the diffraction effects. Taking into account these two competing considerations, there exists an optimal shell length that minimizes the field curvature while preventing the diffraction effects from dominating the image quality. Given the short wavelengths of X-rays and the state of the art of X-ray telescope making, the optimal shell length is on the order of 100 mm at the present time[29].

The grazing incidence nature of X-ray optics requires the mirror to be as thin as possible to maximize aperture utilization efficiency. It also means that an X-ray telescope of a reasonable photon-collecting areas requires a large mirror surface area. For example, the *Chandra* X-ray telescope, which has a photon-collecting area of 0.08 m^2, has a total mirror surface area of 19 m^2, to be compared with the Hubble Space Telescope's 4.5 m^2. The proposed *Lynx* X-ray telescope, with a photon-collecting area of 2 m^2 at 1 keV, requires a total mirror surface area of 372 m^2, equivalent to a 22 m in diameter ground-based telescope.

Our current development effort is further divided into four distinct technology elements: (1) mirror substrate fabrication, (2) coating, (3) alignment, and (4) bonding, each of which is described in detail in Section 4. Table 1 maps the desired properties of an X-ray mirror assembly to the requirements of the four technology elements. The successful implementation of an X-ray telescope lies in a comprehensive optimization of these variables in a specific scientific, technological, budgetary, and spaceflight opportunity context. The objective of our technology development is to advance the four technology elements to ever favor the optimization toward better and more capable science performance for a given set of cost and spaceflight opportunity limitations. The maturity and efficiency of these four technology elements translate directly into schedule and cost reduction of making a mirror assembly, thereby enabling the making of the most powerful telescope in terms of photon-collecting area for the same amount of resources.

Table 1. Mapping of relationships between the desired characteristics (topmost row) of a mirror assembly and the four technology elements (leftmost column) required to build it. These relationships are multi-dimensional. A successful mirror assembly represents a useful compromise among these variables that can be implemented in a specific scientific, technological, spaceflight opportunity, and budgetary context.

	Point-Spread-Function	**Photon-Collecting Area**	**Field of View**	**Energy Bandwidth**	**Production Cost**
Substrate Fabrication	Maximize figure quality, minimize micro-roughness. Optimize substrate length: longer substrates lead to lower diffraction, whereas shorter ones lead to better off-axis PSF.	Minimize areal density and geometric thickness to maximize mirror area for a given mass, and to minimize blockage by mirror thickness.	Minimize substrate length in optical axis direction without sacrificing figure quality.	Minimize micro-roughness to reduce scattering and maximize reflectance. Must be able to make thin mirror substrates.	Minimize metrology requirement. Implement mass production process. Maximize use of commercial technology and materials.
Coating	Maximize X-ray reflectance without degrading figure or micro-roughness.	Maximize X-ray reflectance by maximizing coating density.	Maximize critical reflection angle.	Deposit efficient multi-layer coating without degrading figure or micro-roughness.	Simplify coating process to minimize labor and time.
Alignment	Fully realize potential of each mirror segment.	Minimize loss of photons due to alignment errors.	Locate and orient each mirror segment to achieve best FOV.	Able to align mirror segments that are close together to accommodate small graze angles.	Implement maximum automation to minimize labor and time.
Bonding	Attach mirror segments permanently without degrading figure or alignment.	Minimize space required for bonding mechanism to minimize structural blockage.	Able to bond mirror segments that are far apart from each other without losing mechanical strength to accommodate large graze angles.	Able to bond mirror segments that are close to each other.	Minimize labor and time and maximize reliability of bonding.

4. TECHNOLOGY ELEMENTS

4.1. Fabrication of Mirror Substrates[30]

We have chosen direct fabrication as the method for making mirror segments for two reasons. First, of all the techniques that have been used for making optics in general and X-ray optics in particular, direct fabrication—also known as grind-and-polish—makes the best possible optics. Second, direct fabrication technology has progressed by leaps and bounds in the last 20 years since the *Chandra* mirrors were fabricated in the 1990s. Many then-esoteric techniques have matured and become commercially available in the form of turnkey machines. In particular, ion beam figuring technology has become widely used in the semiconductor industry for making high-precision wafers to meet ever more stringent device fabrication requirements. Perhaps most important of all, some of these polishing processes exert little to no shear stress or normal pressure on the substrate being polished, making it possible to fabricate thin optics without breakage.

In conjunction with choosing the direct fabrication method, we have chosen monocrystalline silicon as the mirror material for several reasons. First of all, monocrystalline silicon is practically free of internal stress, unlike other materials that are full of internal stress because of domain boundaries between crystal grains (as in metals) or because of super-cooling (as in glass). This lack of internal stress makes it possible to use the deterministic material removal techniques to make precision optics: any figure change is determined and only determined by the removal of material. In contrast, for a material with internal stress, the removal of material causes figure change in two ways: (1) the disappearance of the material itself and (2) the disappearance or appearance of stress as a result of the material removal. The figure change due to stress is unpredictable. While an unpredictable, stress-induced figure change is totally negligible for a thick (~10 mm) substrate, it is not so for a thin (~0.5 mm) substrate.

Second, silicon has highly desired material properties. It has a relatively low density of 2.33 g/cm^3, lower than most glasses and aluminum. Its elastic modulus, 150 GPa, is twice that of the typical glass and aluminum alloys, making it stiff. Equally important is its high thermal conductivity, 150 W/mK at room temperature, is more than 100 times higher than typical glass, minimizing thermal gradients caused by the hostile thermal environment of space. Compounding the benefit of high thermal conductivity is its low coefficient of thermal expansion, 2.6 ppm/K at room temperature, lower than typical glass and much lower than typical metals. All of these material properties make silicon almost the ideal material for making X-ray mirrors for spaceflight. It would be ideal if its coefficient of thermal expansion were zero.

In addition, monocrystalline silicon is an industrial material. Large blocks of it are commercially available at low costs. Together with this material availability is the availability of a large body of knowledge accumulated in the last 50 years as well as industrial equipment for processing it by the semiconductor industry. No other material enjoys these advantages. A key aspect of this technology development is to maximize the use of these advantages to make the best X-ray optics at the lowest possible cost.

Once the fabrication technique and material are determined, the thickness of the mirror segment is determined by three parameters: (1) mass allocated for the mirror assembly, (2) mirror surface area, and (3) density of the material. For the proposed *Lynx* mission, for example, these three parameters lead to a thickness of 0.5 mm. The mirror substrate fabrication process, illustrated in Figure 2, starts with a commercially procured block of monocrystalline silicon measuring 150 mm x 150 mm x 75 mm, shown in the upper-left panel. In the next step, (upper-middle panel), a conical approximation contour is cut into the block. The surface is then lapped to generate a precision conical surface that is a zeroth and first order approximation to an X-ray mirror segment. Then, a thin silicon shell is sliced off of the block, as illustrated in upper-right panel. This silicon shell, because of the cutting and lapping process, has damage to its crystal structure. To remove the damage, it is etched in a standard industrial process with a solution of hydrofluoric acid, nitric acid, and acetic acid. After this etching step, the thin shell is a single crystal where practically every atom is on its lattice location. The entire shell is virtually free of internal stress. At this point, the shell's surface is matte and not yet capable of reflecting X-rays.

Then, the conical substrate is polished on a cylindrical tool to achieve required specularity and micro-roughness. In order for the reciprocation to be random in both the circumferential and axial directions to avoid grooving, the conical substrate is elastically bent into a cylindrical shape. This is equivalent to the stress-polishing process that was successfully used for making aspheric mirrors for the Keck telescopes. This step results in a mirror substrate whose clear aperture is approximately 100 mm x 100 mm, with roll-off errors near the four edges that are typical of full-aperture polishing processes, shown in the lower-middle panel of Figure 2. The areas near the edges are then removed, resulting in a mirror substrate of the required size, shown in the lower-right panel. The monocrystalline nature of the substrate is such that the figure of the remaining mirror does not change as a result of the operation after the damage caused by the cutting process is properly removed. The damage along the cut edges is removed via etching.

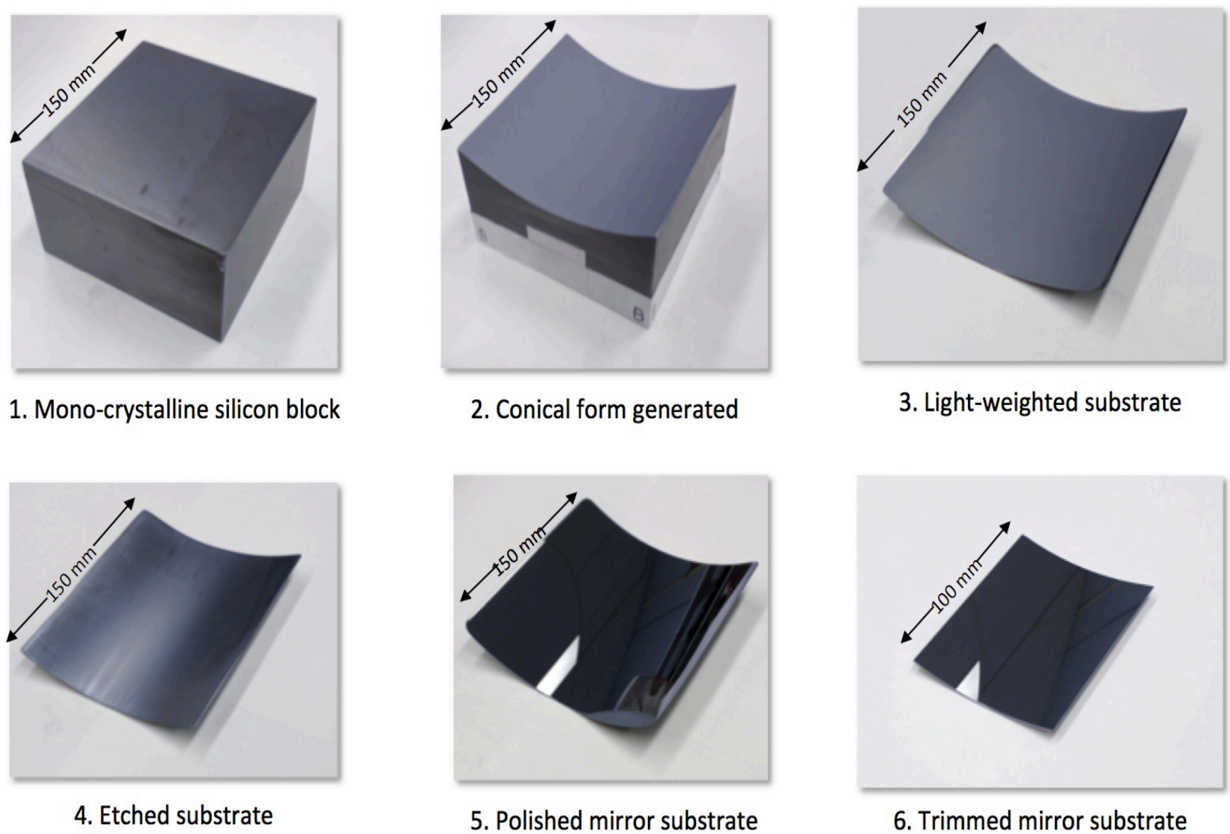

Figure 2. Six major steps of fabricating a mirror substrate. This entire process, using no special equipment other than what is commonly available in the commercial market, takes less than 20 hours of labor time and one week of calendar time. The process is highly amenable to automation and mass production, making possible high throughput and low cost.

The final step of the mirror substrate fabrication is a figuring process using an ion beam. The mirror substrate is measured on an interferometer to produce a topographical map that is used to guide the ion beam to preferentially remove material where the surface is high. As of August 2019, mirror substrates have been fabricated repeatedly and have consistently met *Lynx* requirements. Figure 3 shows the parameters of one of the mirror substrates. Its overall quality is similar to *Chandra's* mirrors. Two mirrors like this one, when properly aligned, are predicted to achieve images of 0.4-arcseconds HPD at 1 keV. In the coming years, every step of the entire substrate fabrication process will be examined, refined, and perfected to achieve better substrates, reaching the diffraction limit by sometime in the late 2020s.

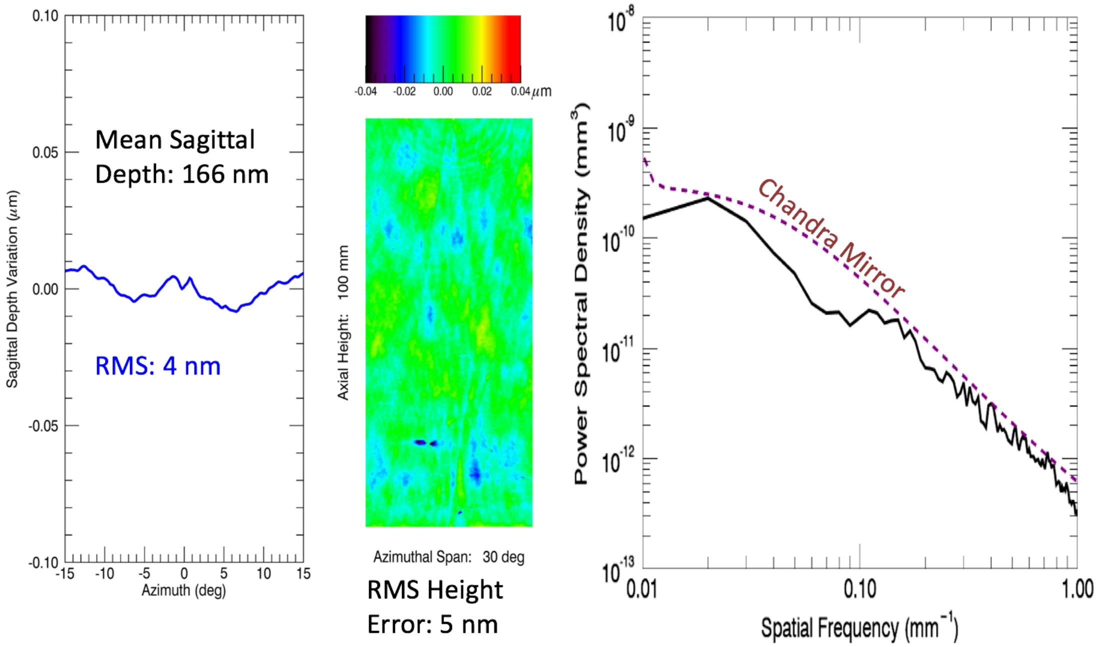

Figure 3. Measured properties of a finished mirror substrate. *Left panel*: Sagittal depth variation as a function of azimuth. This substrate's average sagittal depth of 166 nm differs from the design value of 174 nm by 8 nm. The RMS variation of the sagittal depth is 4 nm. *Middle panel*: Surface error topography. After removal of the sagittal depth, this mirror has an RMS height error of 5 nm. *Right panel*: Power spectral density (black solid curve) in comparison with *Chandra's* mirror (purple dashed curve). All of the errors combine to make this mirror substrate have an image quality of 0.4 arcseconds HPD (two-reflection equivalent).

4.2. Mirror Coating[31]

Bare silicon is a poor X-ray reflector. It must be coated with thin films to enhance its reflectivity. There are potentially many different ways of coating a bare silicon surface to achieve high reflectance, but for the purpose of this technology development, we assume the use of the traditional iridium coating. Other coatings, when fully demonstrated, can be implemented with little to no change to the process presented here. The major issue related to coating is that coating introduces stress that severely distort the figure of a mirror substrate. The preservation of the substrate figure requires a way to cancel or otherwise compensate for the effect caused by the coating stress.

The coating process, shown in Figure 4(a), starts with a bare silicon substrate cleaned of particulate and molecular contaminants. Using the standard semiconductor industry's dry oxide growth process, the backside (i.e., the convex side or the non-reflecting side) is coated with a layer of silicon oxide. The silicon oxide exerts compressive stress on the substrate, causing it to distort as shown in Figure 4(b). Then a thin film of iridium, with an undercoat of chrome serving as a binding layer, is sputtered on the front side. The compressive stress of the iridium film counteracts the silicon oxide stress, cancelling some of the distortion (shown in Figure 4(c)), but still significant distortion remains. The final step (shown in Figure 4(d)) is to trim the thickness of the SiO_2 layer to achieve precise balance of stresses and restore the figure of the substrate. The trimming is guided by precise figure measurement and finite element analysis.

One way of trimming the thickness of the silicon oxide layer is using chemical etching, which has been recently demonstrated[31]. Another way is using an ion beam, the same as figuring the silicon substrate. Since this is a dry process, as opposed to the wet chemical etching process, it has the advantage of being cleaner. It is expected that this will start experimenting with trimming the oxide with an ion-beam in 2019.

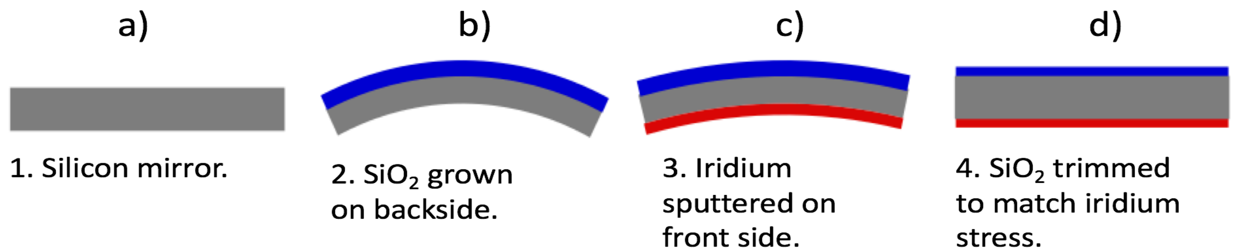

Figure 4. Illustration of the mirror coating process to enhance X-ray reflectance while preserving the figure quality of the silicon substrate. The distortion caused by the stress of the iridium thin film is precisely balanced by the stress of the silicon oxide on the other side of the mirror substrate.

4.3. Mirror Alignment[32]

A mirror segment must be aligned and bonded to form part of a mirror module. A mirror segment will be supported at four optimized locations, as shown in Figure 5. Four supports, as in the case of three supports for a flat mirror, *necessarily* and *sufficiently* determine the location and orientation of a curved mirror such as an X-ray mirror. Using gravity (i.e., the weight of the mirror segment) as the nesting force, the alignment of the mirror segment is determined by the heights of the four supports, which are interchangeably called “posts” or “spacers.” The alignment task is reduced to the precision grinding of the heights of these spacers.

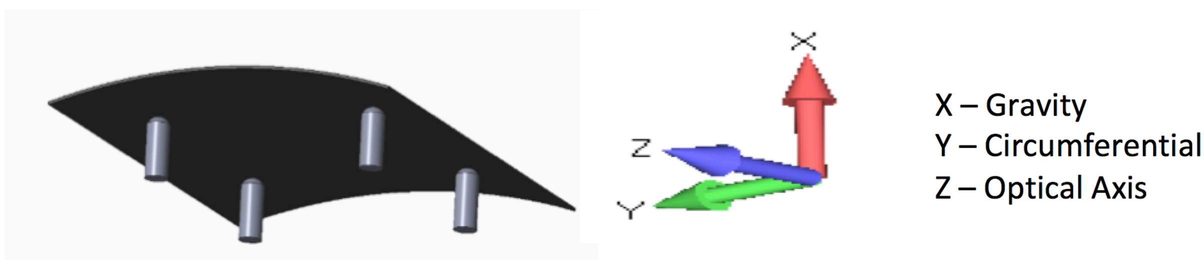

Figure 5. Illustration of the 4-point kinematic support of an X-ray mirror. The four supports, also known as spacers or posts, are approximately located one quarter of the way inboard from each corner. See text for a discussion of the advantages of aligning and bonding a mirror segment using these four supports.

The alignment process is an iteration of Hartmann measurements using a beam of visible light monitored by a CCD camera (shown in Figure 6) and precision grinding of the heights of the spacers. The precision of the spacer heights required depends on the radius of curvature of the mirror segment. In the worst case for *Lynx* for the largest radius of curvature of 1,500 mm, the 0.1-arcsecond alignment error translates into a spacer height error of 25 nm. With a deterministic material removal process, this precision is easily achievable. Over the course of the last two years, many mirror segments have been repeatedly aligned—both primary and secondary ones individually and primary and secondary segments combined—achieving alignment accuracy of approximately 1-arcsecond HPD, which is dominated by the diffraction effects of the visible light. The plan forward is to refine this process by using visible light of a shorter wavelength to minimize the diffraction effect to achieve 0.1-arcsecond alignment precision.

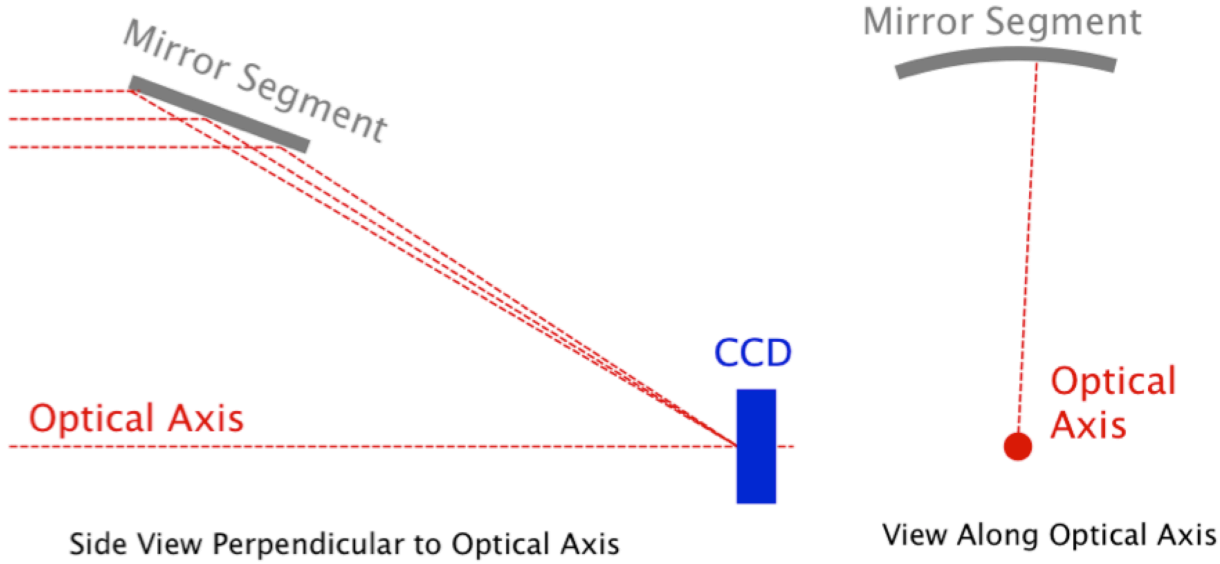

Figure 6. Illustration of the Hartmann setup using a beam of visible light to measure the location and orientation of the mirror segment being aligned.

4.4. Mirror Bonding[32]

Bonding the mirror segment is a direct extension of the alignment process. Once the four spacers have the correct heights as determined by the Hartmann measurement, the mirror segment is removed, epoxy is applied to the top of each of the four spacers, and then the mirror segment is placed on them again. Finally, vibration is applied to help the mirror segment settle in its optimal configuration, the same way as during the iterative alignment process. During the settling process, because of the weight of the mirror and the vibration, the epoxy on each spacer is spread and compressed such that the top of the spacer touches the mirror. The mirror segment is permanently bonded when the epoxy has cured.

Supporting and bonding the mirror segment in this way has many advantages. First, the gravity-induced distortion is not frozen in permanently. Because of the optimization of the locations of the four spacers, the gravity distortion disappears once the gravity is released. Second, the epoxy bonds do not affect the alignment of the mirror segment. Third, any local distortion caused by epoxy cure is minimal, as the diameter of the spacer is only a few times larger than the thickness of the mirror segment. The mirror segment, being 0.5 mm in thickness, is stiff over the length scale of several millimeters similar to the diameter of the spacers.

The validity of the entire process, from mirror substrate fabrication to alignment and bonding, has been demonstrated through successful repeated building and testing of mirror modules, as shown in Figure 7. A module was placed in the 600-m X-ray beam line at NASA Goddard Space Flight Center and produced images with 1.2-arcseconds HPD, as shown in the right panel. A similar module was tested at the Panter 100-m X-ray beamline and measured for its effective areas at several different energies, agreeing within 2% with calculations based on atomic form factors measured independently.

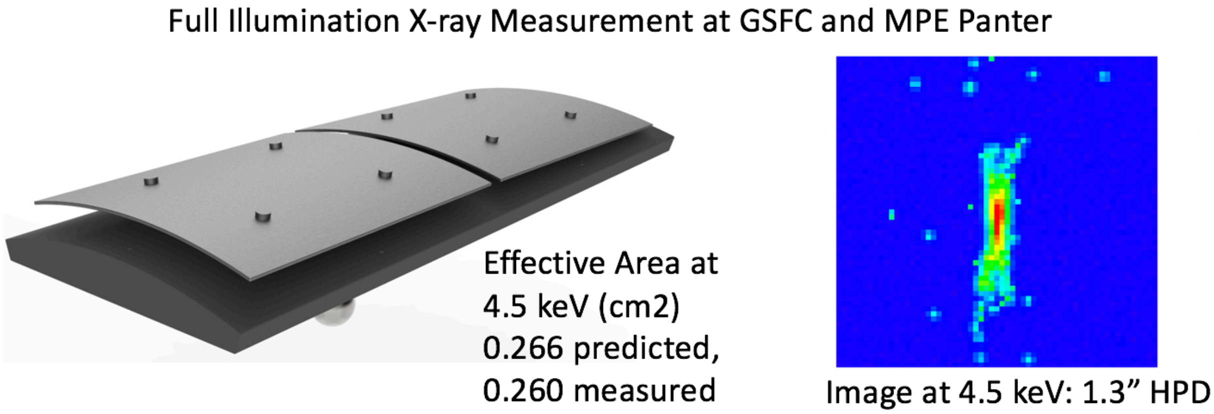

Figure 7. *Left:* A pair of mirror segments aligned and bonded on a silicon plate. Each mirror is bonded at four locations with silicon spacers (not visible in this view). The four spacers on the back of each of the two mirrors are there for the next pair of mirror segments. *Right:* An X-ray image obtained with a beam of 4.5-keV (Ti K) X-rays with a half-power diameter of 1.2 arcseconds. The effective areas at several energies are measured of a similarly built module at MPE’s Panter X-ray beam line, thanks to Dr. Vadim Burwitz and his team, to agree with theoretical expectations.

5. FUTURE WORK

The approach described in this paper, based on precision polishing of mono-crystalline silicon, has had an excellent beginning and has undergone rapid progress in the last few years. Among other things, we have shown that it is likely that this technology will enable the realization of the dream of X-ray astronomers to have an observatory that has better PSF and many times more photon-collecting area than the Chandra X-ray Observatory. While much has been achieved, more remains to be done. We expect that in the next few years we will continue our work in the all technology areas. In particular, we will place more emphasis on systems engineering[33] as technology elements become more mature. We will continue to refine the mirror substrate fabrication process to make better substrates and simplify the process to reduce fabrication time and thereby reduce fabrication cost. We expect to fully realize the Wolter-Schwarzschild prescription. Once demonstrating the coating process using iridium, we will proceed to coat substrates with interference coatings that have the potential of increasing the photon-collecting areas of a typical mirror assembly by more than 20% at a minimal cost.

Most important of all, we will build and test, both for science performance and spaceflight environment, mirror modules with progressively more mirror segments to mature the alignment and bonding process to achieve not only good PSF, but also structural robustness against vibration, acoustic, and shock tests. We will also progress toward planning and understanding and addressing logistical issues associated with making and qualifiying a larger number of modules[34].

ACKNOWLEDGEMENTS

The authors wish to acknowledge the work of the many people who have helped advance this technology. Especially we want to thank Dr. Vadim Burwitz and his team at the Panter X-ray Beam Facility at the Max Planck Institute for Extraterrestrial Physics in Garching, Germany, who conducted many X-ray tests and measurements of our mirror modules, helping us identifying problems and devising solutions. The work has been funded by NASA through the Astronomy & Physics Research and Analysis Program (APRA) and the Strategic Astrophysics Technology Program under the Research Opportunities in Space and Earth Sciences (ROSES) program.

REFERENCES

[1] Giacconi, R. & Rossi, B., "*A telescope for soft X-ray astronomy*," J. Geophys. Res., Vol. 62, p. 773 (1960).

[2] Young, P.S., "*Fabrication of the high resolution mirror assembly for the HEAO 2 telescope*," SPIE Proc. Vol. 194, p. 131 (1979).

[3] Aschenbach, B., "*Design, construction, and performance of the ROSAT high-resolution x-ray mirror assembly,*" Appl. Opt., Vol. 27, p. 1404 (1988).

[4] VanSpeybroeck, L.P., "*Performance Expectation versus Reality*," SPIE Proc. Vol. 3113, p. 89 (1997).

[5] Gondoin, P., et al., "*X-ray multi-mirror (XMM) telescope*," SPIE 2279, 86-100 (1994).

[6] Gaskin, J.A., et al., "*The Lynx X-ray observatory: concept study overview and status,*" SPIE Proc., Vol. 10699, p. 106990N (2018).

[7] Mushotzky, R.F., et al., "*AXIS: a probe class next generation high angular resolution x-ray imaging satellite*," SPIE Proc., Vol. 10699, p. 1069929 (2018).

[8] Astrophysical Transient Probe (ATP) website: https://asd.gsfc.nasa.gov/tap/

[9] Madsen, K., et al., "*The high-energy X-ray probe*," SPIE Proc., Vol. 10699, 10699B (2018)

[10] McClelland, R.S., et al., "*The STAR-X X-ray telescope assembly*," SPIE Proc., Vol. 10399, p. 1039908 (2017).

[11] Nakazawa, K., et al., "*The FORCE mission: science aim and instrument parameter for broadband X-ray imaging spectroscopy with good angular resolution,*" SPIE Proc., Vol. 10699, p. 106992D (2018).

[12] Boella, G., et al., "*The medium-energy concentrator spectrometer on board the BeppoSAX X-ray astronomy satellite,*" A & A Supplement series, Vol. 122, p.327-340 (1997).

[13] Burrows, D.N., et al., "*Swift X-ray Telescope,*" SPIE Proc. Vol. 4140, p. 64 (2000).

[14] Arcangili, L., et al., "*The eROSITA X-ray mirrors: technology and qualification aspects of the production of mandrels, shells and mirror modules*," SPIE Proc., Vol. 10565, p. 1056558 (2017).

[15] De Kort, P.A.J., *et al., "The X-Ray Imaging Telescopes On EXOSAT,"* Space Sci. Rev., Vol. 30, 495, (1981).

[16] Serlemitsos, P. J., et al. "*The x-ray telescope onboard Suzaku*," PASJ 59, pp. 9-21 (2007).

[17] Craig, W.W., et al., "*Fabrication of the NuSTAR Flight Optics*," SPIE Proc. Vol. 8147, p. 81470H-1 (2011).

[18] Zhang, W.W., et al., "*High-resolution, lightweight, and low-cost x-ray optics for the Lynx observatory*," JATIS, Vol. 5, id. 021012 (2019).

[19] Zhang, W.W., et al., *"Next generation X-ray optics: high-resolution, light-weight, and low-cost,"* A paper submitted to NASA in response to solicitation NNH11ZDA018L (2011).

[20] Zhang, W.W., et al., "*Next generation astronomical X-ray optics: high angular resolution, light weight, and low production cost*," SPIE Proc., 8443, p. 84430S (2012).

[21] Zhang, W. W., et al., "*High resolution and high throughput x-ray optics for future astronomical missions*," SPIE Proc., Vol. 8861, p. 88610N (2013).

[22] Zhang, W. W., et al., "*Affordable and lightweight high-resolution x-ray optics for astronomical missions*," SPIE Proc., Vol. 9144, p. 914415 (2014).

[23] Zhang, W.W., et al., "*Toward diffraction-limited lightweight x-ray optics for astronomy,*" SPIE Proc, Vol. 9603, p. 96030Q (2015).

[24] Zhang, W.W., et al., "*Lightweight and high-resolution single crystal silicon optics for x-ray astronomy*," SPIE Proc., 9905, p. 99051S (2016).

[25] Zhang, W.W., et al., "*Monocrystalline silicon and the meta-shell approach to building X-ray astronomical optics*," SPIE Proc., Vol. 10399, p. 103990S (2017).

[26] Zhang, W.W., et al., "*Astronomical x-ray optics using mono-crystalline silicon: high resolution, light weight, and low cost,*" SPIE Proc., Vol. 10699, p. 106990O (2018)

[27] Zhang, W.W., et al., "*High-resolution, lightweight, and low-cost x-ray optics for the Lynx observatory*," JATIS, Vol. 5, p. 021012-1 (2019).

[28] Saha, T.T., "*General surface equations for glancing incidence telescopes*," Appl. Opt., Vol. 26, p. 658 (1987).

[29] Saha, T.T., et al., "*Design optimization for x-ray telescopes*," in these proceedings.

[30] Riveros, R.E., et al., "*Fabrication of Monocrystalline Silicon X-ray Mirrors*," in these proceedings.

[31] Yao, Y., et al., "*Progress of coating stress compensation of silicon mirrors for Lynx x-ray telescope mission concept using thermal oxide patterning method*," JATIS, Vol. 5, p. 021011-1 (2019).

[32] Chan, K.W., et al., "*Recent Advances in the Alignment and Bonding of Silicon Mirrors for High-Resolution Astronomical X-ray Optics*," in these proceedings.

[33] Solly, P.M., "*Structural analysis and testing of silicon x-ray mirror modules*," in these proceedings (2019).

[34] Biskach, M.P., et al., "*Mass manufacturing of high resolution and lightweight monocrystalline silicon mirror modules,*" in these proceedings (2019).